

Interstellar H₂ toward HD 147888

Gnaciński Piotr

Institute of Theoretical Physics and Astrophysics,
University of Gdańsk, ul. Wita Stwosza 57, 80-952 Gdańsk,

Received January 14, 2013/ Accepted January 14, 2013

Abstract

The ultraviolet and far-ultraviolet spectra of HD 147888 allows to access the $\nu=0$ as well as higher vibrational levels of the ground H₂ electronic level. We have determined column densities of the H₂ molecule on vibrational levels $\nu=0-5$ and rotational levels $J=0-6$. The ortho to para H₂ ratio for the excited vibrational states equals to 1.2. For the lowest vibrational state $\nu = 0$ and rotational level $J=1$ the ortho to para H₂ ratio is only 0.16. The temperature of ortho–para thermodynamical equilibrium is $T_{OP} = 43 \pm 3$ K.

The large number of H₂ absorption lines in the HST spectra allows to determine column densities even from a noisy spectra. The measurements of H₂ column densities on excited vibrational levels (from the HST spectra) leads to constrains of radiation field in photon–dominated regions (PDR) models of interstellar cloud towards HD 147888.

Key words: *ISM: clouds – ISM: molecules – Ultraviolet: ISM*

1 Introduction

The molecular hydrogen is the most common molecule in the interstellar medium. First detection of H₂ on vibrationally excited levels was per-

formed by Federman *et al.* (1995) in HST (Hubble Space Telescope) spectrum of ζ Oph. A rich spectrum of vibrationally excited hydrogen molecule was described by Meyer *et al.* (2001) in the HST STIS (Space Telescope Imaging Spectrograph) spectrum of HD 37903. They have also noticed that vibrationally excited H₂ is present in the cloud towards HD 147888.

The presence of both FUSE (Far Ultraviolet Spectroscopic Explorer) and HST STIS spectra for HD 147888 (ρ Oph D) gives us a rare opportunity to measure column density of H₂ energy levels excited by fluorescence ($\nu > 0$) and also by collisions ($\nu=0$). In a consequence we can calculate a PDR model which is well constrained by density and by the ultraviolet radiation flux (star–cloud distance).

2 Observations

We have used HST STIS spectrum o59s05010 to obtain column densities on vibrationally excited H₂ levels. The STIS spectrum consists of 2 subexposures which were combined into a single spectrum ranging from 1160 Å to 1356.8 Å. The column densities of the ground vibrational levels ($\nu''=0$) were determined from the FUSE spectra P1161501016-19. These spectra were averaged using the IRAF tasks *pooffsets* and *specalign*. The FUSE spectrum extends

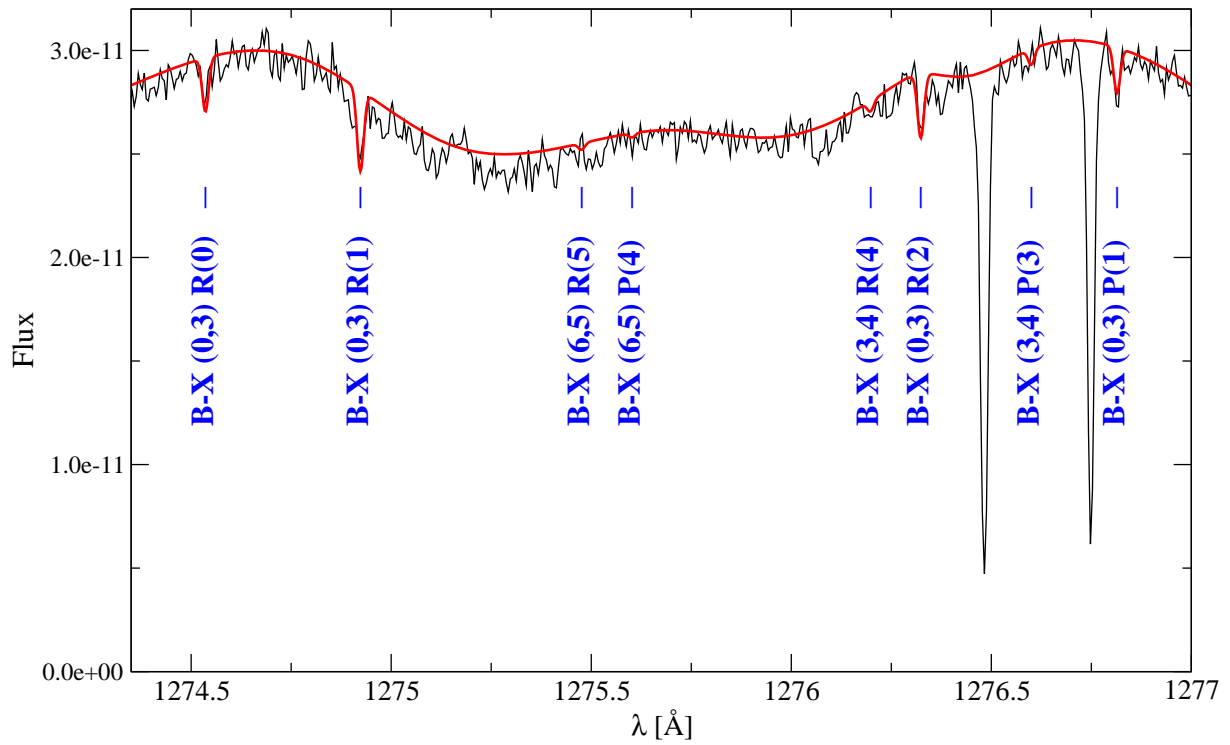


Figure 1: A fragment of the HST spectrum. The synthetic spectrum (red line) was fitted to the whole HST spectrum. The Doppler broadening parameter was set to $b = 2.5$ km/s. The two deep absorption lines are CI lines.

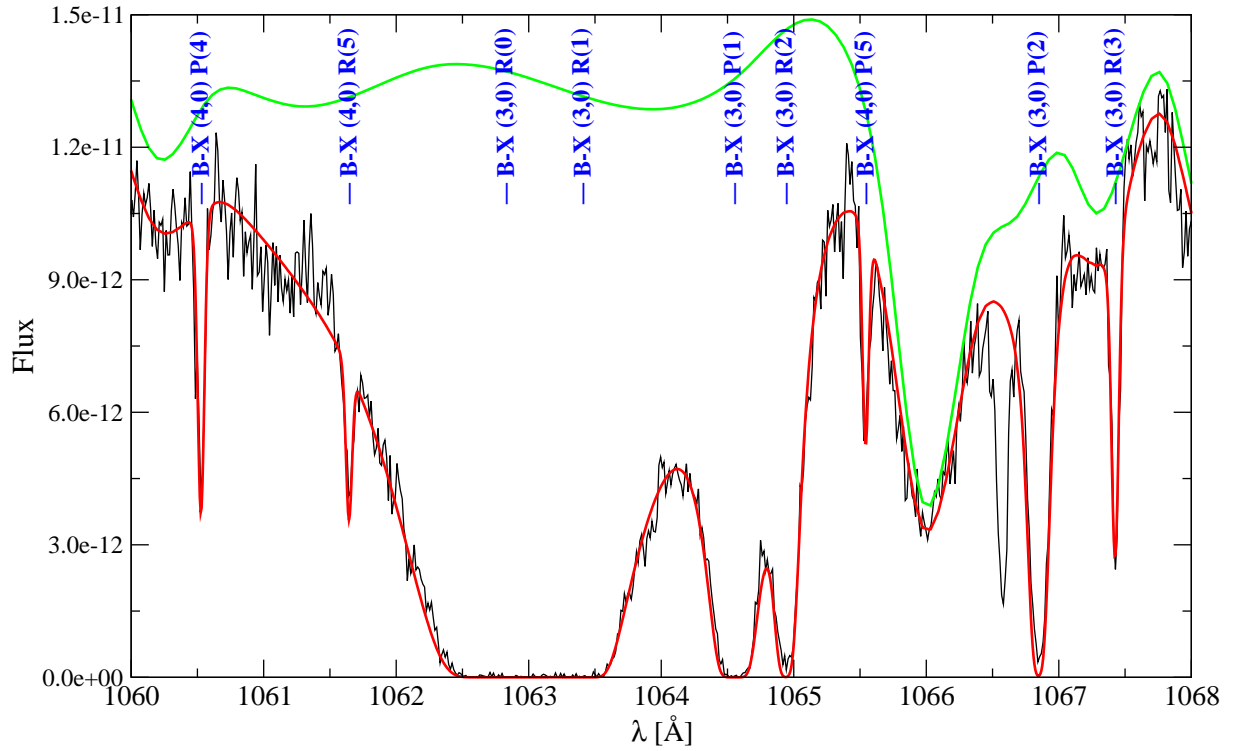


Figure 2: A fragment of FUSE spectra with the B–X (3,0) transitions of H₂. The green line represents continuum and the red one is the simulated spectrum fitted to the observed one (black line). The absorption line at 1066.66 Å is an Ar I line.

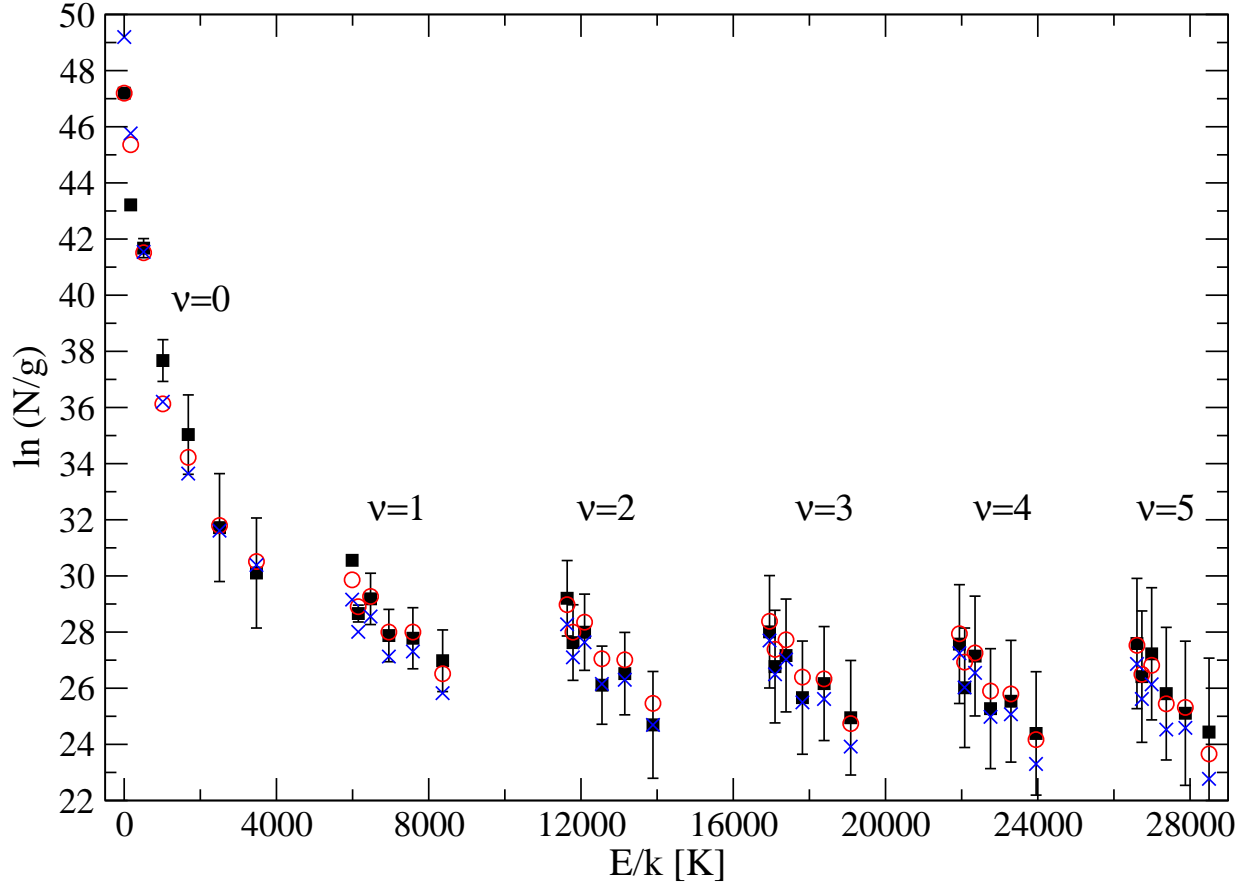


Figure 3: Natural logarithms of H_2 column densities divided by statistical weight plotted versus energy (squares with error bar). The ν symbol denotes the vibrational quantum number. For $\nu=0$ rotational quantum numbers are $J=0-6$, and for vibrationally excited levels ($\nu > 0$) $J=0-5$. The first PDR cloud model is shown as red circles. The second model is shown as blue crosses.

from 904 Å to 1188 Å. We have used FUSE spectra from the following detectors 1blif4, 2alif4 and 1alif4 which have the best quality.

The whole HST STIS spectrum was fitted at once with a synthetic spectrum consisting of 355 H₂ absorption lines. The cloud velocity and column densities of all vibrationally excited levels were free parameters. The H₂ spectral line positions and oscillator strengths were adopted from Abgrall *et al.* (1994). A fragment of HST spectrum together with a fit to the whole HST spectrum is shown on fig. 1.

Each transition from ground $\nu=0$ $J=0,1$ levels to vibrationally excited levels of the B electronic level were fitted independently in the FUSE spectrum. We have calculated column densities from the following transitions: (0,0), (1,0), (2,0), (3,0) and (4,0). The first digit in parentheses denotes the upper vibrational level of the B electronic state. The second digit (always 0) is the vibrational level of the ground electronic level X. At each point of the synthetic spectrum optical depth of spectral lines lying no more than 30 Å were summed. The point spread function (PSF) for the FUSE spectra was a Gauss function with FWHM=15 km/s (Jensen *et al.* (2010)). The natural line widths were given by Abgrall *et al.* (2000). A synthetic spectrum together with the FUSE observation is shown on fig. 2. The derived molecular hydrogen column densities are presented in table 1 and shown on fig. 3.

3 Noise robustness

Some of the H₂ absorption lines in the HST spectrum are at the noise level (eg. absorption lines from the $\nu = 1$ level). Therefore we have tested the robustness of the fit against noise. The noise observed on the HST STIS spectrum is about 1% at 1360 Å and 3% at 1160 Å. We have added Gaussian noise of amplitude A to the best fit synthetic spec-

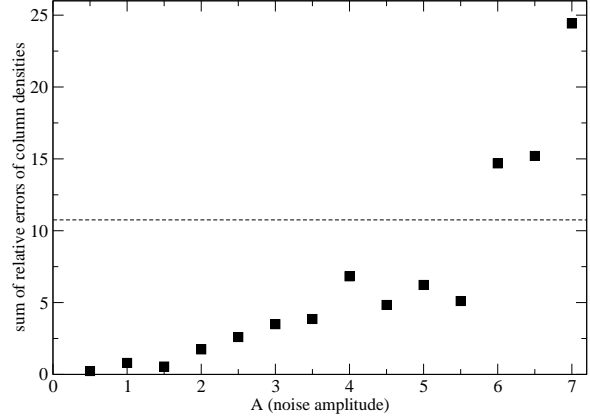


Figure 4: Robustness of the synthetic spectrum fit to the noisy data. The dashed line shows errors introduced by changing the original column densities by 60% (close to the quoted errors of column densities).

trum. The points of the generated noisy spectrum are at the same wavelengths as the HST spectrum used previously in the fitting procedure. The Gaussian noise has standard deviation $\sigma = 1$. The spectrum with noise was generated using the formula $F_A = F_{fit}(1 + A(-0.01\lambda + 14.6) \cdot 0.01 \cdot \text{GaussianNoise})$, where the factor $(-0.01\lambda + 14.6)\%$ reflects the changing noise amplitude in the original HST spectrum. The amplitude $A = 1$ reflects the noise level in the original HST spectrum. The F_{fit} is a synthetic spectrum that represents the best fit to the observed HST STIS spectra.

Next we have performed a fit to the generated spectrum F_A and obtained new column densities by fitting a new synthetic spectrum to the noisy one. All fits to the noisy spectrum were performed with Doppler broadening parameter fixed to $b = 2.5$ km/s. The cloud velocity and all column densities for $\nu \geq 1$ were free parameters. The continuum level was common for all fits. In order to evaluate the error introduced by noise of various magnitude A we have cal-

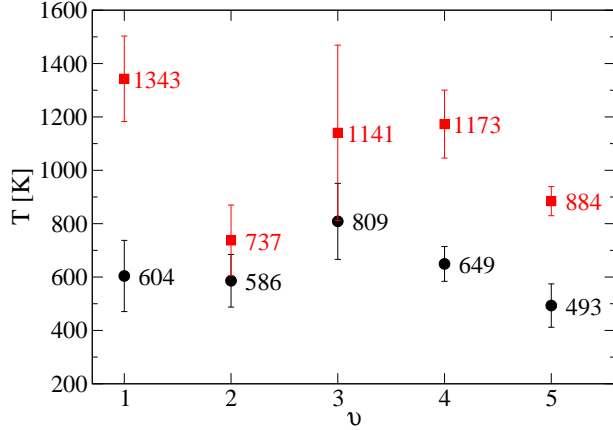


Figure 5: The rotational temperature on vibrational levels 1–5. Red squares presents rotational temperature of ortho H_2 , while the black circles are for para- H_2 .

culated a sum of squared relative errors:

$$\sum_{v \geq 1, J=0-5} \left(\frac{N_A(v, J) - N_0(v, J)}{N_0(v, J)} \right)^2. \quad (1)$$

The symbol N_A represents column density calculated from spectrum with noise amplitude A . The results are shown on fig. 4. Even for the noise amplitude 5.5 times larger then in the HST spectra the resulting column densities errors are significantly less to the 60 % errors in the best fit column densities. Errors about 60 % are common for H_2 column densities derived from the HST spectra (see tab. 1). So the fitting procedure is very robust against the noise. Note however, that if the original HST spectrum had the noise 5 times larger, then the continuum placement would be problematic or even impossible.

4 Temperatures

The total observed column density of molecular hydrogen is equal to $N(H_2) = (3.74 \pm 0.36) \cdot 10^{20}$. The

column density of atomic hydrogen $N(HI) = (5.7 \pm 1.1) \cdot 10^{21} \text{ cm}^{-2}$ was determined by Cartledge *et al.* (2006). The resulting molecular fraction of hydrogen $f(H_2) = 2N(H_2)/(N(HI) + 2N(H_2)) = 0.11 \pm 0.02$. The ortho-para H_2 ratio for vibrational levels $v \geq 1$ is $O/P = 1.23 \pm 0.21$. However the ortho-para H_2 ratio on the $v=0, J=1$ level is significantly lower. It was calculated using the method presented by Wilgenbus *et al.* (2000) and is equal to $0.16^{+0.04}_{-0.02}$.

The temperature of ortho-para H_2 equilibrium T_{OP} was derived from the equation:

$$\frac{N(1)}{N(0)} = \frac{g(1)}{g(0)} \exp\left(-\frac{E(1) - E(0)}{kT_{OP}}\right), \quad (2)$$

where $N(J)$ are the column densities, $E(J)$ is the energy on the J level ($v=0$) and $g(J)$ is the statistical weight

$$g(J) = \begin{cases} (2J+1) & \text{for para } H_2 \text{ (even } J) \\ 3(2J+1) & \text{for ortho } H_2 \text{ (odd } J). \end{cases} \quad (3)$$

The temperature of ortho-para H_2 equilibrium $T_{OP} = 43 \pm 3 \text{ K}$, similar to the value $T_{OP} = 45 \pm 3 \text{ K}$ derived by Jensen *et al.* (2010).

The T_{02} rotational temperature involves only para- H_2 levels and was calculated from equation analogous to eq. 2. The T_{02} rotational temperature equals to $92 \pm 7 \text{ K}$ (Jensen *et al.* (2010) gives $T_{02} = 88 \pm 1 \text{ K}$).

The rotational temperature was also calculated for each vibrational level. The rotational temperature is the inverse of line inclination taken with the minus sign on a plot: $\ln(N/g)$ versus E/k (see fig. 3). The line inclination was calculated with the linear regression method separately for ortho and para H_2 spin isomers. The resulting temperatures are presented on fig. 5. The vibrational level $v=0$ is populated by both collisions and fluorescence and cannot be fitted with a single temperature.

For each excited vibrational level the points on the $\ln(N/g)$ versus E/k plot (fig. 3) are perfectly

Table 1: Column densities of the H₂ ro-vibrational levels towards HD 147888 [log cm⁻²]. The absorption lines connected with the column densities marked in bold were clearly seen in the spectrum. Other lines are at the noise level.

$J \setminus v$	0	1	2	3	4	5
0	20.50 ± 0.04	13.27 ± 0.05	12.68 ± 0.58	12.16 ± 0.87	11.97 ± 0.92	11.98 ± 1.01
1	19.72 ± 0.08	13.40 ± 0.13	12.95 ± 0.58	12.58 ± 0.87	12.25 ± 0.92	12.43 ± 1.02
2	18.80 ± 0.15	13.37 ± 0.40	12.86 ± 0.59	12.50 ± 0.87	12.49 ± 0.93	12.52 ± 1.02
3	17.68 ± 0.32	13.43 ± 0.40	12.66 ± 0.60	12.47 ± 0.88	12.30 ± 0.93	12.53 ± 1.03
4	16.17 ± 0.61	13.02 ± 0.47	12.47 ± 0.64	12.32 ± 0.88	12.04 ± 0.94	11.86 ± 1.12
5	15.29 ± 0.83	13.24 ± 0.48	12.24 ± 0.83	12.35 ± 0.89	12.11 ± 0.95	12.13 ± 1.14
6	14.19 ± 0.85	—	—	—	—	—

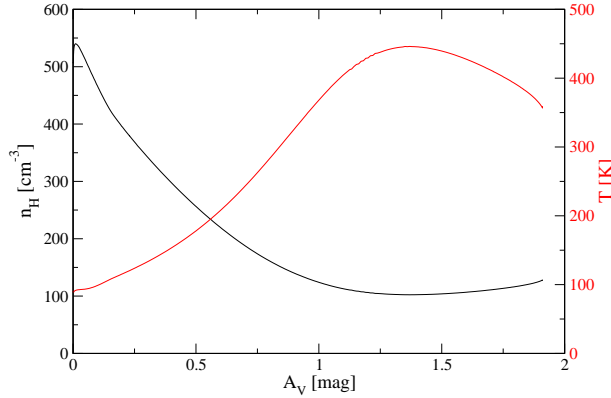


Figure 6: The hydrogen density and kinetic temperature in the first cloud model (at d=0.44 pc).

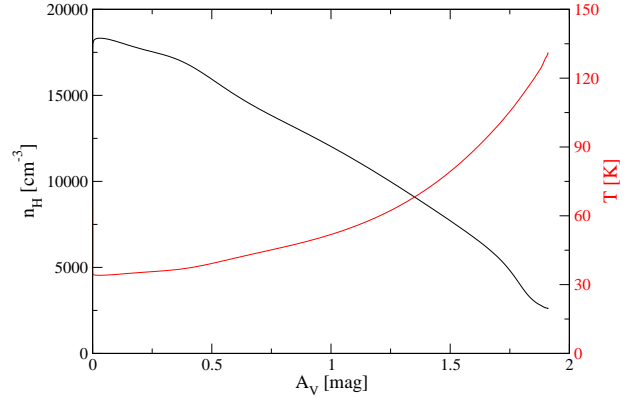


Figure 7: The hydrogen density and kinetic temperature in the second cloud model (at d=0.99 pc).

placed on a straight line (separately ortho and para states). The correlation coefficient is between 0.92 and 0.996. The agreement with the Boltzmann distribution confirms the correctness of the H₂ column densities.

5 Models

We have used the Meudon PDR code (Le Petit *et al.*, 2006) to calculate the model of interstellar cloud in front of HD 147888. We have calculated isobaric models with exact radiative transfer in all H₂ spectral lines. The interstellar radiation field on the ob-

server side was always 1 Draine unit. The turbulent velocity was set to $v_{turb}=2$ km/s and the star spectral type to B3V. The interstellar reddening $E(B-V)=0.47$, $R_V=4.06$ and $A_V=1.91$ were adopted from Rachford *et al.* (2009).

The first PDR model was chosen among 1290 models by minimizing the difference of relative H₂ abundances observed in the cloud towards HD 147888 and calculated in a PDR model:

$$\sum_{v,J} w_v \left(\log \frac{N_{obs}(v, J)}{N_{obs}(0, 0)} - \log \frac{N_{model}(v, J)}{N_{model}(0, 0)} \right)^2 \quad (4)$$

The weights w_v were chosen so, that the levels usually excited by fluorescence ($v > 0$) have the some

influence on the final sum, as the $\nu = 0$ level excited collisionally. The weights w_ν were equal to 5 for $\nu=0$ and 1 otherwise.

The first PDR model has a star–cloud distance of 0.44 pc. The interstellar radiation field on the star side is equal to 500 Draine units. The hydrogen density varies from 127 cm^{-3} on the star side to 539 cm^{-3} near the observers side. The gas kinetic temperature changes from 359 K on the star side to 90 K on the observer’s cloud side. In this cloud model the ortho/para H_2 ratio for vibrationally excited states equals to 1.5.

Our second model was selected by minimizing the difference between the observed and calculated column densities:

$$\sum_{\nu, J} w_\nu (\log N_{obs}(\nu, J) - \log N_{model}(\nu, J))^2 \quad (5)$$

A model chosen using the above formula has to reproduce the H_2 column densities. Our attempts to find a model satisfying the formula led to an unphysical model for the cloud in front of HD 37903. However we decided to present such model of the cloud towards HD 147888 for comparison purposes, as it has the hydrogen density at the observer side close to the density presented by Jensen *et al.* (2010). The PDR model presented by Jensen *et al.* (2010) has $n_H=2000 \text{ cm}^{-3}$. However, this model did not take into account the H_2 molecules in excited vibrational levels ($\nu > 0$).

In the second model the hydrogen density varies from $n_H = 18300 \text{ cm}^{-3}$ near the observers side to $n_H = 2604 \text{ cm}^{-3}$ on the star side. The temperature changes from $T = 34 \text{ K}$ to $T = 131 \text{ K}$, and the interstellar radiation field on the star side is 1 Draine unit. The star–cloud distance in the second model is 0.99 pc. The ortho/para H_2 ratio in the cloud model equals to 1.4 and the total H_2 column density equals to $3.0 \cdot 10^{21} \text{ cm}^{-2}$. Column densities of H_2 energy levels in both models are shown on fig. 3.

6 Conclusions

The ortho–para H_2 ratio on excited vibrational levels ($(O/P)_{\nu>0} = 1.2$) differs from the O/P H_2 on the ground vibrational level ($(O/P)_{\nu=0, J=1} = 0.16$).

It is possible to obtain column densities from large number of shallow absorption lines arising from the same ground level. The whole HST STIS spectrum should be fitted at once with a synthetic spectrum to derive column densities from a noisy spectrum.

Acknowledgments

This research was supported by University of Gdańsk grant BW/5400-5-0336-0. I would like to thank Herve Abgrall for providing the natural line widths for the H_2 lines.

References

- Abgrall H., Roueff E., Drira I., 2000, A&ASS, **141**, 297
- Abgrall H., Roueff E., Launay F., Roncin J.-Y., 1994, Can. J. Phys., **72**, 856
- Cartledge S.I.B. *et al.*, 2006, ApJ, **641**, 327
- Federman S.R. *et al.*, 1995, ApJ, **445**, 325
- Jensen A., Snow T., Sonneborn G., Rachford B., 2010, ApJ, **711**, 1236
- Le Petit F., Nehmé C., Le Bourlot J., Roueff E., 2006, ApJSS, **164**, 506
- Meyer D.M. *et al.*, 2001, ApJ, **553**, L59
- Rachford B.L. *et al.*, 2009, ApJSS, **180**, 125
- Wilgenbus D. *et al.*, 2000, A&A, **356**, 1010